First-principles study of the conduction-electron-mediated interactions between nuclear spins in copper metal

A. S. Oja
Low Temperature Laboratory, Helsinki University of Technology, SF-02150 Espoo, Finland

X. W. Wang* and B. N. Harmon
Ames Laboratory–U.S. Department of Energy, Iowa State University, Ames, Iowa 50011
(Received 26 September 1988)

Motivated by recent success in observing the ordering of copper nuclei at very low temperatures, we have used first-principles electronic structure calculations to evaluate the conduction-electron-mediated coupling strengths between the nuclear spins. Scalar-relativistic wave functions from a self-consistent linear augmented-plane-wave calculation were used to evaluate the contact, dipolar, and orbital electron-nuclear interactions. Besides the isotropic Ruderman-Kittel coupling between nuclei, the electron-nuclear dipolar and orbital interactions give rise to significant anisotropic coupling terms. The symmetry of the anisotropic coupling is not dipolar in form and the significance of this for analysis of NMR line broadening is pointed out. The coupling strengths are in good agreement with various NMR measurements. Using mean-field theory, the overall coupling predicts an ordering wave vector at $(2\pi/a)(0.87,0,0)$ and a helical spin structure; however, this state is only 0.6% lower in energy than the state with ordering vector $(2\pi/a)(1,0,0)$, which is the one recently observed in neutron scattering experiments. The numerical calculations are not precise enough to accurately determine the ordering vector because of this extremely small difference in energy for states near the zone boundary along the (1,0,0) direction.

I. INTRODUCTION

In some remarkable experiments utilizing a double-stage nuclear demagnetization refrigerator, the magnetic ordering of copper nuclei was observed at a 58-nK nuclear-spin temperature.[1] The measured susceptibility indicated an antiferromagnetic ground state, and very recent neutron scattering experiments have confirmed this.[2] The coupling between the nuclear spins in a nonmagnetic metal, like copper, arises from both dipole-dipole interactions and the indirect interactions mediated by the conduction electrons. Unlike most electronic systems, the resulting spin Hamiltonian is amenable to detailed quantitative analysis so that these experiments may herald the beginning of a new chapter in the study of magnetism. Indeed, these ideal local moment systems with the possibility of isotopic substitution for introducing disorder could provide the best experimental realizations of many tractable mathematical models. In this paper we examine the conduction-electron-mediated indirect interactions. These have traditionally been studied using a free-electron model along the lines first suggested by Ruderman and Kittel,[3] with the strength of the interactions dependent on an empirical parameter whose value is determined by NMR measurements. Besides the contact interaction considered by Ruderman and Kittel, orbital and dipolar electron-nuclear interactions are also present.[4] We have adopted modern electronic-structure techniques to evaluate all of these electron-nuclear interactions and thereby obtain the full nuclear-nuclear coupling strengths starting from first principles. Besides presenting our numerical results, we assess the present state of the theory regarding the indirect interactions. This seems particularly appropriate in view of the new experimental results. We also discuss in this paper the symmetry of the interaction which differs somewhat from that used in previous studies that invoked simplifying assumptions about the band structure. A brief account of our earlier work concerning the dominant contact interaction has been reported.[5] In Sec. II we develop the formalism describing the indirect-coupling Hamiltonian, starting with the electron-nuclear interaction. The numerical methods are briefly described in Sec. III, while the results are presented in Sec. IV. The discussion of the ordered spin structure based on mean-field theory is given in Sec. IV C, and the conclusions and discussions are contained in the last section.

II. FORMALISM

A. Hyperfine Hamiltonian

There are three closely related phenomena in metals which arise from the hyperfine interaction between a nucleus and conduction electrons: the Knight shift, nuclear-spin relaxation, and indirect conduction-electron-mediated nuclear-spin interactions. Although quantitative understanding of the Knight shift and nuclear-spin relaxation has been achieved in several metals, the same level of understanding has not yet been realized for indirect interactions. While this paper is mainly concerned with indirect interactions, we calculate other

quantities related to the hyperfine interaction in order to obtain an overall understanding of the hyperfine phenomena in the same material. We also use these related phenomena to test that our wave functions and matrix elements yield a consistent picture.

The hyperfine Hamiltonian between an electron and a nucleus, in a nonrelativistic theory, consists of three parts:

$$H_{\text{el-n}}=H_{\text{el-n}}^{\text{cont}}+H_{\text{el-n}}^{\text{dip}}+H_{\text{el-n}}^{\text{orb}} , \tag{1}$$

where the different terms are called contact, dipolar, and orbital interactions, respectively.

The contact interaction depends on the charge density of electrons at the nuclear site

$$H_{\text{el-n}}^{\text{cont}}=\frac{8\pi}{3}\hbar^2\gamma_e\gamma_n\delta(\mathbf{r})\mathbf{I}\cdot\mathbf{S} , \tag{2}$$

and therefore only s electrons contribute to it. In atoms which have one unpaired s-electron (or a large polarization of core s electrons due to exchange between electrons and an unfilled shell), $H_{\text{el-n}}^{\text{cont}}$ manifests itself in the hyperfine splitting of atomic levels. (For a review of electron-nuclear interactions in atoms we refer the reader to Lindgren and Rosen.[6]) In several cases, the hyperfine splitting has been used to estimate the magnitude of hyperfine induced effects in a metal. This can be justified if one limits oneself only to some column in the Periodic Table, like Cu, Ag, and Au, since then the s-electron densities are expected to rescale roughly in the same way inside the column as one goes from an atom to a metal.[7] This method has been used to estimate the magnitude of indirect coupling in Au.[8]

The other two terms in the hyperfine Hamiltonian, the dipolar and the orbital, are only from electrons which have a nonspherical charge density. The dipolar part is

$$H_{\text{el-n}}^{\text{dip}}=-\hbar^2\gamma_e\gamma_n r^{-3}[\mathbf{I}\cdot\mathbf{S}-3(\mathbf{I}\cdot\hat{\mathbf{r}})(\mathbf{S}\cdot\hat{\mathbf{r}})] . \tag{3}$$

The minus sign results from our choice of a positive γ_e. When calculating the matrix elements of $H_{\text{el-n}}^{\text{dip}}$, we have found it convenient to expand in terms of spherical harmonics.[9]

$$H_{\text{el-n}}^{\text{dip}}=\sum_{\alpha}\hbar^2\gamma_e\gamma_n I^{\alpha *}\phi_{\text{dip}}^{\alpha}(\mathbf{S},\mathbf{r}),\quad \alpha=-,z,+ , \tag{4}$$

where we have introduced a basis (I^-,I^z,I^+) instead of (I^x,I^y,I^z) using the well-known transformation

$$I^{\pm}=I^x\pm iI^y . \tag{5}$$

The functions $\phi_{\text{dip}}^{\alpha}(\mathbf{S},\mathbf{r})$ are

$$\phi_{\text{dip}}^{\pm}(\mathbf{S},\mathbf{r})=r^{-3}\left[\frac{4\pi}{5}\right]^{1/2}[\mp(\tfrac{3}{2})^{1/2}Y_2^{\pm 1}(\hat{\mathbf{r}})S^z-\tfrac{1}{2}Y_2^0(\hat{\mathbf{r}})S^{\pm} +(\tfrac{3}{2})^{1/2}Y_2^{\pm 2}(\hat{\mathbf{r}})S^{\mp}] \tag{6a}$$

and

$$\phi_{\text{dip}}^{z}(\mathbf{S},\mathbf{r})=r^{-3}\left[\frac{4\pi}{5}\right]^{1/2}[2Y_2^0(\hat{\mathbf{r}})S^z+(\tfrac{3}{2})^{1/2}Y_2^{-1}(\hat{\mathbf{r}})S^+ -(\tfrac{3}{2})^{1/2}Y_2^1(\hat{\mathbf{r}})S^-] . \tag{6b}$$

We introduce a general notation

$$\phi_{\text{dip}}^{\alpha}(\mathbf{S},\mathbf{r})=r^{-3}\left[\frac{4\pi}{5}\right]^{1/2}\sum_{\gamma}c(\gamma,\alpha)Y_2^{m(\gamma,\alpha)}(\hat{\mathbf{r}})S^{\gamma} ,\quad \gamma=-,z,+ . \tag{7}$$

Equations (6a) and (6b) define the values of $c(\gamma,\alpha)$ and $m(\gamma,\alpha)$. Because the terms contain $Y_2^m(\hat{\mathbf{r}})$, the dipolar interaction only couples states whose partial-wave numbers l,l' satisfy $l-l'=0,\pm 2$.

The orbital part of the hyperfine Hamiltonian is

$$H_{\text{el-n}}^{\text{orb}}=\hbar^2\gamma_e\gamma_n r^{-3}\mathbf{I}\cdot\boldsymbol{l} , \tag{8}$$

where $\boldsymbol{l}$ is the orbital-angular-momentum operator. In a crystal with inversion symmetry, the orbital-angular-momentum matrix elements $\langle\mathbf{k}\nu|l_z|\mathbf{k}\nu\rangle$ are zero (here ν is the band index). In the calculation of spin-lattice relaxation and for the indirect interaction, the off-diagonal matrix elements $\langle\mathbf{k}\nu|l_z|\mathbf{k}'\nu'\rangle$ are involved in the second-order perturbation theory, and their contribution can be large. In copper, the orbital mechanism contributes roughly 20% to the spin-lattice relaxation rate,[10] which led us to investigate whether the orbital terms also would make such a large contribution to indirect coupling. Indeed, in a model calculation, which employed the so-called Bardeen's spherical approximation for conduction-electron wave functions, orbital terms were found to contribute significantly to indirect coupling.[11]

Since copper is a light element, relativistic effects are, in general, unimportant for the electronic structure of the metal; however, the $l=0$ radial functions are modified significantly near the nucleus by relativistic corrections. We have included the dominant contributions by using a self-consistent scalar-relativistic method which neglects spin-orbit coupling but includes all other effects such as the mass enhancement and Darwin terms.[12] We continue to describe the formalism using the nonrelativistic form of the interactions which are more transparent and are suitable for application to copper if the radial matrix elements are treated properly.[13]

B. Indirect-coupling Hamiltonian

The hyperfine interaction between an electron and a nucleus gives rise to a coupling of two nuclear spins, as was found originally by Ruderman and Kittel.[3] In second-order perturbation theory, the effective Hamiltonian coupling two spins i and j becomes

$$H_{ij}=\sum_{\mathbf{k},\nu,\sigma}\sum_{\mathbf{k}',\nu',\sigma'}\frac{\langle\mathbf{k}\nu\sigma|H_{\text{el-n}}^{i}|\mathbf{k}'\nu'\sigma'\rangle\langle\mathbf{k}'\nu'\sigma'|H_{\text{el-n}}^{j}|\mathbf{k}\nu\sigma\rangle}{\varepsilon(\mathbf{k},\nu,\sigma)-\varepsilon(\mathbf{k}',\nu',\sigma')}f(\mathbf{k},\nu,\sigma)[1-f(\mathbf{k}',\nu',\sigma')]+\text{c.c.} , \tag{9}$$

where $\mathbf{k}$ is the wave vector, ν the band index, and σ the spin of a conduction electron. The energy $\varepsilon(\mathbf{k},\nu,\sigma)=\varepsilon(\mathbf{k},\nu)$ in our case, where the ground state has no spin polarization. The function $f(\mathbf{k},\nu,\sigma)=f(\varepsilon(\mathbf{k},\nu))$ is the Fermi function. In the above equation the electronic states are summed over, so that H_{ij} describes coupling between the nuclear degrees of freedom.

Since we neglect the spin-orbit coupling, the cross terms between the spin and orbital induced interactions vanish. The remaining modes of interactions are described by the following matrix elements (using a transparent short-hand notation):

$$\langle H_{\text{el-n}}^{\text{cont}}\rangle\langle H_{\text{el-n}}^{\text{cont}}\rangle \rightarrow \text{ Ruderman-Kittel (RK), } H_{ij}^{\text{RK}} ,$$

$$\langle H_{\text{el-n}}^{\text{cont}}\rangle\langle H_{\text{el-n}}^{\text{dip}}\rangle \rightarrow \text{ pseudodipolar (PD), } H_{ij}^{\text{PD}} ,$$

$$\langle H_{\text{el-n}}^{\text{dip}}\rangle\langle H_{\text{el-n}}^{\text{dip}}\rangle \rightarrow \text{ tensor-tensor (TT), } H_{ij}^{\text{TT}} ,$$

$$\langle H_{\text{el-n}}^{\text{orb}}\rangle\langle H_{\text{el-n}}^{\text{orb}}\rangle \rightarrow \text{ orbital (orb), } H_{ij}^{\text{orb}} .$$

On the right-hand side we have indicated the name and abbreviation of the corresponding indirect-coupling mode that we use in this paper. We are following the original nomenclature by Bloembergen and Rowland,[4] which was based on the symmetry properties of the coupling modes in the spin space and is awkward for the two terms involving $H_{\text{el-n}}^{\text{dip}}$.

As a consequence of the fact that

$$\sum_{\sigma,\sigma'}\langle\sigma|\mathbf{S}\cdot\mathbf{I}_i|\sigma'\rangle\langle\sigma'|\mathbf{S}\cdot\mathbf{I}_j|\sigma\rangle=\tfrac{1}{2}\mathbf{I}_i\cdot\mathbf{I}_j , \tag{10}$$

the RK interaction is isotropic in spin space. In the free-electron approximation, the RK interaction takes a simple form:

$$H_{ij}^{\text{RK}}\propto r_{ij}^{-3}[\cos(2k_F r_{ij}) - \sin(2k_F r_{ij})/(2k_F r_{ij})]\mathbf{I}_i\cdot\mathbf{I}_j . \tag{11}$$

The interaction is oscillatory and of long range. These general features were also found in two recent first-principles calculations of the RF interaction in copper.[5,14,15]

The rest of the coupling modes cause an anisotropic coupling between nuclear spins. Bloembergen and Rowland were the first to discuss these modes.[4] By employing the so-called Bardeen's spherical approximation[16] for conduction-electron wave functions, they found that the pseudodipolar interaction has the form

$$H_{ij}^{\text{PD}}=B_{ij}^{\text{PD}}[\mathbf{I}_i\cdot\mathbf{I}_j-3(\hat{\mathbf{r}}_{ij}\cdot\mathbf{I}_i)(\hat{\mathbf{r}}_{ij}\cdot\mathbf{I}_j)] , \tag{12}$$

where the range function $B_{ij}^{\text{PD}}=B^{\text{PD}}(r_{ij})$ is oscillatory and of long range. For the tensor-tensor interaction, Bloembergen and Rowland found the form

$$H_{ij}^{\text{TT}}=A_{ij}^{\text{TT}}\mathbf{I}_i\cdot\mathbf{I}_j+B_{ij}^{\text{TT}}[\mathbf{I}_i\cdot\mathbf{I}_j-3(\hat{\mathbf{r}}_{ij}\cdot\mathbf{I}_i)(\hat{\mathbf{r}}_{ij}\cdot\mathbf{I}_j)] , \tag{13}$$

where the range functions A_{ij}^{TT} and B_{ij}^{TT} depending on r_{ij} are again oscillatory and of long range. Complete analytical expressions for the range functions within the spherical approximation have been given by Oja and Kumar who also considered the orbital coupling and found that H_{ij}^{orb} can be decomposed in a way similar to H_{ij}^{TT} as given in Eq. (13).[11]

However, there is no reason for the anisotropic coupling to have the dipolarlike symmetry in spin space as was pointed out already by Abragam.[17] As we will show, the form of the anisotropic coupling is determined by the symmetry of the crystal.

C. Symmetry properties

Generally, the Hamiltonian which couples two spins can be written as

$$H_{ij}=-(I_i^x I_i^y I_i^z)\cdot\begin{bmatrix} a & d+\tilde{d} & e-\tilde{e} \\ d-\tilde{d} & b & f+\tilde{f} \\ e+\tilde{e} & f-\tilde{f} & c \end{bmatrix}\cdot\begin{bmatrix} I_j^x \\ I_j^y \\ I_j^z \end{bmatrix} , \tag{14}$$

where the matrix elements are guaranteed to be real by the addition of the complex conjugate in Eq. (9). Each element is explicitly written as a sum of the symmetric and antisymmetric parts. Equation (14) can be rewritten as

$$H_{ij}=-\mathbf{I}_i\cdot\underline{A}_{ij}\cdot\mathbf{I}_j-\mathbf{D}_{ij}\cdot\mathbf{I}_i\times\mathbf{I}_j , \tag{15}$$

where $\underline{A}_{ij}$ is the symmetric part

$$\underline{A}_{ij}=\begin{bmatrix} a & d & e \\ d & b & f \\ e & f & c \end{bmatrix} , \tag{16}$$

and $\mathbf{D}_{ij}=(\tilde{f},\tilde{e},\tilde{d})$ describes the antisymmetric Dzyaloshinski-Moriya interaction which is known to play a role in spin glasses, for example. In crystals with inversion symmetry, the case we are considering is $\mathbf{D}_{ij}=0$. However, in a real sample, $\mathbf{D}_{ij}$ will always be nonzero near crystal imperfections, impurities, and surfaces.

Now we consider the form of $\underline{A}_{ij}$ assuming the crystal has inversion symmetry. If the vector $\mathbf{r}_{ij}$ joining the i and j sites lies in some symmetry direction, there exists a non-unit point group operation $\hat{\boldsymbol{\beta}}$ which leaves $\mathbf{r}_{ij}$ invariant, i.e., $\hat{\boldsymbol{\beta}}\mathbf{r}_{ij}=\mathbf{r}_{ij}$. Thus,

$$\underline{A}_{ij}=\underline{A}(\mathbf{r}_{ij})=\underline{A}(\hat{\boldsymbol{\beta}}\mathbf{r}_{ij})=\hat{\boldsymbol{\beta}}\underline{A}_{ij}\hat{\boldsymbol{\beta}}^{-1} , \tag{17}$$

where the last equality follows from the fact that $\underline{A}(\mathbf{r}_{ij})$ transforms like a second rank tensor with respect to $\mathbf{r}_{ij}$, which can be verified by a direct calculation starting from Eq. (9). Depending on the symmetry of $\mathbf{r}_{ij}$, various restrictions are imposed on elements of $\underline{A}_{ij}$. For a cubic lattice, we have the following six possibilities:

$$\mathbf{r}_{ij}\|[l00],\quad \underline{A}_{ij}=\begin{bmatrix} a & 0 & 0 \\ 0 & b & 0 \\ 0 & 0 & b \end{bmatrix} , \tag{18a}$$

$$\mathbf{r}_{ij}\|[ll0],\quad \underline{A}_{ij}=\begin{bmatrix} a & d & 0 \\ d & a & 0 \\ 0 & 0 & c \end{bmatrix} , \tag{18b}$$

$$\mathbf{r}_{ij}\|[lll],\quad \underline{A}_{ij}=\begin{bmatrix} a & d & d \\ d & a & d \\ d & d & a \end{bmatrix}, \tag{18c}$$

$$\mathbf{r}_{ij}\|[lm0],\quad \underline{A}_{ij}=\begin{bmatrix} a & d & 0 \\ d & b & 0 \\ 0 & 0 & c \end{bmatrix}, \tag{18d}$$

$$\mathbf{r}_{ij}\|[llm],\quad \underline{A}_{ij}=\begin{bmatrix} a & d & e \\ d & a & e \\ e & e & c \end{bmatrix}, \tag{18e}$$

$$\mathbf{r}_{ij}\|[lmn],\quad \underline{A}_{ij}=\begin{bmatrix} a & d & e \\ d & b & f \\ e & f & c \end{bmatrix}. \tag{18f}$$

It can be seen that depending on the symmetry of $\mathbf{r}_{ij}$, the number of independent parameters for the anisotropic coupling is different. If the anisotropic coupling could be decomposed into an isotropic and dipolelike part, as in Eq. (13), the number of independent parameters would always be two. From the above we see that this is the case only when $\mathbf{r}_{ij}$ is in the $[l00]$ or $[lll]$ direction.

The underlying reason for Bloembergen and Rowland's original result that the anisotropic interaction can always be decomposed into an isotropic and a dipolelike part is in their use of the spherical approximation for conduction-electron wave functions. Then the interaction is invariant under arbitrary rotations R about $\mathbf{r}_{ij}$, $\underline{A}_{ij}=R\underline{A}_{ij}R^{-1}$, instead of a finite set of rotations $\hat{\beta}$ dictated by the crystal. This results exactly in a decomposition into isotropic and dipolelike parts for $\underline{A}_{ij}$, as in Eq. (13). We discuss consequences of the full interaction symmetry on the interpretation of NMR line shape analysis in Appendix A.

III. METHODS AND COMPUTATIONAL DETAILS

For a meaningful evaluation of the indirect coupling, it is important to start with an accurate calculation of the electronic structure (both energy bands and wave functions). We have adopted the linearized augmented-plane-wave (LAPW) technique to obtain a self-consistent potential for Cu. The standard local-density approximation (LDA) is used to reduce the complicated (and unknown) exact exchange-correlation energy to a tractable single-particle type of potential. This approximation is known to be remarkably successful in many electronic structure applications, however, it should be used with some caution for evaluation of densities near the nucleus where there is a strong inhomogeneity in the electronic density.[18] We have also used a muffin-tin approximation for the potential. For close-packed metals, this is a good approximation which has minimal effect on the wave functions near the nucleus. To make contact with previous work, we first calculated the nonrelativistic band structure and charge densities which are essentially identical with the Cu results reported by Moruzzi, Janak, and Williams (MJW) using the same potential and approximations.[19] As mentioned in the Introduction, relativistic effects are important, and our later calculations for the evaluation of the indirect coupling were made with eigenvalues and wave functions obtained using exactly the same techniques, but with radial functions evaluated by a self-consistent, scalar-relativistic method.[12] The band structure (i.e., energy eigenvalues) is little affected by the relativistic corrections. For speed in evaluating the $\mathbf{q}$-dependent matrix elements, the wave functions and eigenvalues in the $\frac{1}{48}$th irreducible section of the Brillouin zone were calculated once and stored in a large data base.

Before evaluating Eq. (9) for the indirect coupling, it is worthwhile to investigate independently the spin-lattice relaxation and the Knight shift, both of which involve electronic matrix elements with the hyperfine interaction. In order to assess the size of relativistic corrections and make contact with previous calculations we evaluated the spin-lattice relaxation and Knight shift both nonrelativistically and relativistically. The numerical convergence for the $\mathbf{k}$ space summation and the band summation are also important to consider since with the energy denominator alone they are slowly convergent.[14] After discussing these topics below, we give expressions for the indirect coupling matrix elements in terms of the LAPW wave functions.

A. Spin-lattice relaxation and Knight shift

The spin-lattice relaxation involves the hyperfine coupling between nuclei and the electron states at the Fermi level.[9] A calculation of the relaxation rate thus provides a useful test for some of the wave functions and the matrix elements required in evaluating the indirect coupling. The spin-lattice relaxation rate of Cu also has been calculated by two other groups using modern techniques.[10,20] In Appendix B, we give the formulas for the various quantities which enter such a calculation and give a comparison of our results with those previously published. The agreement among the three independent nonrelativistic calculations is excellent; however, the final relaxation rate is about 17% smaller than the experimental value. This discrepancy is largely due to relativistic effects.

The importance of relativistic effects for Cu is perhaps best illustrated by considering the atomic hyperfine splitting.[6,13] The splitting involves $|\psi_{4s}(0)|^2$ in the nonrelativistic formulation, while the corresponding relativistic hyperfine operator is proportional to $\int_0^\infty g(r)f(r)\,dr$, where $g(r)$ and $f(r)$ are the large and small components of the relativistic $4s$ wave function. A self-consistent, relativistic calculation of the hyperfine splitting for atomic Cu gives a value 14% larger than the corresponding nonrelativistic value. [Note that the density at the nucleus, $|\psi_{4s}(0)|^2$, is 41% larger in the relativistic calculation.] Because it is the square of the hyperfine interaction which enters the indirect coupling Hamiltonian, Eq. (9), it is important that relativistic effects be considered. Besides the enhancement of the hyperfine matrix elements for the s component of the wave functions, we also find that the effects of relativity also cause a small change in the relative position of the d and s bands and a slight (but

significant) increase in the density of s-like states at the Fermi level. We find the overall relativistic enhancement for the s-component contribution to the spin-lattice relaxation to be $+34\%$ (see Table IV) while Ebert *et al.*[20] found a 26% enhancement.

It is also worth mentioning that atomic hyperfine splitting calculations using the local-density approximation are not very reliable. The main problem is that at large values of r, the potential falls off exponentially rather than as e^2/r. The Cu $4s$ orbital density is sensitive to the potential in this outer region and in turn the value of the $4s$ orbital density at the nucleus varies when corrections to the potential are attempted at large r. We have found that such variations in $|\psi_{4s}(0)|^2$ can be as large as the effects of including relativity for the hyperfine field. Luckily such difficulties are not a problem in the bulk solid. There still remains, however, the error caused by using the local-density approximation (LDA) for a situation in which the charge density near the nucleus has a large inhomogeneity. We do not believe this is a large error for Cu, given the overall agreement of our results with experiments. Indeed, it will only be through careful calculations and comparison with experiment that a valid assessment of the use of the LDA for hyperfine interactions can be made.

We now turn to the Knight shift. According to the theory first proposed by Townes, Herring, and Knight,[21] the dominant contribution to the Knight shift is given by

$$K=\frac{8\pi}{3}\chi_P\langle|\psi(0)|^2\rangle_{E_F}\ , \tag{19}$$

where χ_P is the Pauli paramagnetic spin susceptibility, and the average is to be taken over the electronic states on the Fermi surface. This can be easily evaluated by noting

$$\left.\frac{\partial\rho(r=0)}{\partial E}\right|_{E_F}=2\sum_k\delta(E_k-E_F)|\psi_k(0)|^2$$
$$\equiv 2n(E_F)\langle|\psi(0)|^2\rangle_{E_F}\ , \tag{20}$$

where $n(E_F)$ is the density of states per Ry spin atom. Using the nonrelativistic values from Table IV we have

$$\left.\frac{\partial\rho(0)}{\partial E}\right|_{E_F}=2n_s(E_F)\frac{|\psi_s(0)|^2}{4\pi}$$
$$=2(0.222\ e/\text{Ry spin})(13.92\ \text{a.u.}^{-3})$$
$$=6.18e/(\text{Ry spin a.u.}^3)\ . \tag{21}$$

This is within 1% of the MJW value.[19] Also from Table IV, $n_{\text{tot}}(E_F)=1.958$ states/Ry spin so we can derive

$$\langle|\psi(0)|^2\rangle_{E_F}=1.578\ \text{a.u.}^{-3}\ .$$

The enhanced χ_P of Eq. (19) is given by $2\mu_B^2 n(E_F)S$, where the Stoner enhancement factor, $S=1.12$, is taken again from the tables of MJW.[19] We therefore obtain a nonrelativistic value for the Knight shift of $K=0.156$, whereas the experimental value is 0.239.[22] We should mention that our nonrelativistic results using the potential of MJW have a systematic error, since their potential was obtained for the theoretical equilibrium-lattice constant of 6.76 a.u. Our self-consistent relativistic calculations were all performed assuming the experimental-lattice constant of 6.83 a.u.

We also evaluated the Knight shift using the results of our self-consistent relativistic calculations. The relativistic value is 0.172, leaving a 39% discrepancy with the experimental value, 0.239. To investigate a possible reason for this discrepancy, we evaluated the orbital contribution to the Knight shift. Walstedt and Yafet were similarly motivated 25 years ago and made a back-of-the-envelope estimate of the orbital Knight shift for Cu.[23] They found $K_{\text{orb}}\simeq 0.25$, but argued that their matrix element estimates were too crude and inaccurate so that K_{orb} was probably closer to 0.06 (which would bring the total Knight shift into agreement with experiment). Using accurate matrix elements and summing over the first nine bands, we find $K_{\text{orb}}\simeq 0.20$. One might argue that the reference salt (CuCl or others) also has some orbital contribution, but we estimate this could only bring the effective K_{orb} down to 0.17. We have also examined the core-polarization contribution using spin polarized atomic calculations and estimate a negative value of around -0.017 or -10% of the Fermi contact term. In any case, the situation now is that the theoretical K_{tot} is 0.34. We suspect that a major cause of this discrepancy with experiment is caused by a large diamagnetic contribution beyond the Larmor contribution which is, of course, also present in the reference salts. This suspicion is strengthened by estimates of the total bulk susceptibility, where we find (in 10^{-6} emu/mole) $\chi_{\text{Pauli}}=10.9$, $\chi_{\text{VanVleck}}=16.6$, and $\chi_{\text{dia}}=-15.6$; yielding $\chi_{\text{tot}}=11.9$, whereas the experimental value is -5.5. The above estimate of χ_{dia} comes from just the Cu core and d^{10} configuration of the ion, leaving the conduction-electron contribution to be a very large -17.4 to get agreement with experiment. To our knowledge, this has never been satisfactorily calculated for Cu and would require a major effort.

In short, we believe the present interpretation of Knight shift data is not complete and further effects have to be considered.

B. k-space summation for indirect interaction

Without the matrix elements, the Fourier transform of Eq. (9) reduces to the expression for the bare susceptibility:

$$\chi^0(\mathbf{q})=\sum_{\mathbf{k},\nu,\nu'}\frac{f(\mathbf{k},\nu)[1-f(\mathbf{k}+\mathbf{q},\nu')]}{\varepsilon(\mathbf{k}+\mathbf{q},\nu')-\varepsilon(\mathbf{k},\nu)}\ , \tag{22}$$

where ν and ν' label the band indices and f is the Fermi-Dirac occupation function. To evaluate this summation, the so-called tetrahedron method is used.[24,25] The Brillouin zone is partitioned into a large number (~ 1000) of small tetrahedrons, and the energy eigenvalues are calculated for the $\mathbf{k}$ points at the four corners of each tetrahedron. Inside each tetrahedon, the energy dispersion is assumed to be linear and the contribution to the susceptibility can be evaluated analytically. As an example, we show in Fig. 1 the results of a numerical calculation of

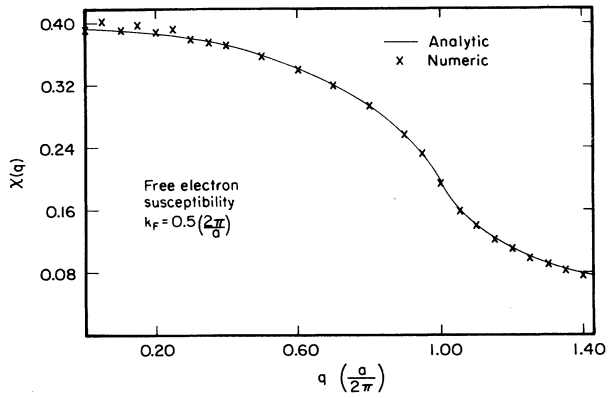

FIG. 1. Susceptibility Eq. (22), using free-electron energy bands. The analytic Lindhard function is compared to the numerical values obtained using the tetrahedron method as described in the text.

$\chi^0(\mathbf{q})$ for the free-electron gas. The corresponding analytical result (Lindhard function) is shown as the solid line. There is some systematic error for small q values, since in this limit, the $f(1-f)$ factors restrict the summation to states near the Fermi level and the mesh of tetrahedra is a bit coarse to give a good representation for the Fermi surface.

C. LAPW matrix elements

Instead of calculating the interaction in real space,

$$H_{ij} = -\sum_{\alpha,\beta} I_i^\alpha A_{ij}^{\alpha\beta} I_j^\beta - \text{c.c.}, \quad \alpha,\beta = x,y,z \ , \tag{23}$$

we calculate the Fourier transform of it,

$$A^{\alpha\beta}(\mathbf{q}) = \sum_j A_{ij}^{\alpha\beta} \exp(i\mathbf{q}\cdot\mathbf{r}_{ij}) \ . \tag{24}$$

We write $A^{\alpha\beta}(\mathbf{q})$ as

$$A^{\alpha\beta}(\mathbf{q}) = \hbar^4\gamma_e^2\gamma_n^2 \frac{1}{N}\sum_{\mathbf{k},\nu}\sum_{\nu'} \frac{f(\mathbf{k},\nu)[1-f(\mathbf{k}+\mathbf{q},\nu')]}{\varepsilon(\mathbf{k}+\mathbf{q},\nu')-\varepsilon(\mathbf{k},\nu)} \times M^{\alpha\beta}(\mathbf{k},\nu,\mathbf{k}+\mathbf{q},\nu') \ , \tag{25}$$

where the sum over electronic-spin states has been performed to obtain $M^{\alpha\beta}(\mathbf{k},\nu,\mathbf{k}+\mathbf{q},\nu')$ from the product of the two matrix elements in Eq. (9). The advantage of calculating $A^{\alpha\beta}(\mathbf{q})$ rather than $A_{ij}^{\alpha\beta}$ is that only one $\mathbf{k}$ sum is needed. The summation was performed by assuming $M^{\alpha\beta}$ to be constant within each small tetrahedron and by using the tetrahedron method for calculating the susceptibility term.[24,25]

The matrix element $M^{\alpha\beta}(\mathbf{k},\nu,\mathbf{k}+\mathbf{q},\nu')$ is decomposed into terms arising from the Ruderman-Kittel, pseudodipolar, tensor-tensor, and orbital interactions

$$M^{\alpha\beta} = M_{\text{RK}}^{\alpha\beta} + M_{\text{PD}}^{\alpha\beta} + M_{TT}^{\alpha\beta} + M_{\text{orb}}^{\alpha\beta} \ . \tag{26}$$

In the following, we give expressions for the various matrix elements in terms of the LAPW wave functions,[26]

$$\phi(\mathbf{k},\nu) = \sum_{l,m} [a_{lm}^\nu(\mathbf{k}) u_l(r) + b_{lm}^\nu(\mathbf{k}) u_l'(r)] Y_{lm}(\hat{\mathbf{r}}) \ , \quad r < R_{\text{MT}} \ , \tag{27}$$

where a_{lm}^ν and b_{lm}^ν are the expansion coefficients for the radial wave function, $u_l(r)$, and its energy derivative $u_l'(r)$.

We neglect the contributions to the matrix elements which come from outside of the muffin-tin sphere. This is correct within 2% because of the relatively short range of the interactions. In order to avoid unwieldy expressions, we drop the $b_{lm}^\nu(\mathbf{k})u_l'(r)$ terms from the three subsequent equations. The expressions will be similar for any method that decomposes the wave functions into angular momentum components.

1. Ruderman-Kittel

$$M_{\text{RK}}^{\alpha\beta}(\mathbf{k},\nu,\mathbf{k}',\nu') = \tfrac{2}{9} a_{00}^\nu(\mathbf{k})^2 a_{00}^{\nu'}(\mathbf{k}')^2 u_0^4(0)\delta_{\alpha\beta} \ , \quad \alpha,\beta = x,y,z \ . \tag{28}$$

The δ function makes the interaction isotropic in spin space.

2. Pseudodipolar

This coupling mode involves both contact and dipolar hyperfine interactions and is therefore proportional to the product of the density of the conduction electrons at the nuclear site and the expectation value of r^{-3}. We define the matrix element of r^{-3} between different partial waves as

$$m_{lml'm'}^{\nu\nu'}(\mathbf{k}') = a_{lm}^{\nu*}(\mathbf{k}) a_{l'm'}^{\nu'}(\mathbf{k}') \int_0^{R_{\text{MT}}} u_l(r) u_{l'}(r) r^{-1} dr \ . \tag{29}$$

Now we can write the pseudodipolar interaction as

$$M_{\text{PD}}^{\alpha\beta}(\mathbf{k},\nu,\mathbf{k}',\nu') = \tfrac{1}{3} u_0^2(0) \sum_{l,m,l',m'} [m_{lml'm'}^{\nu\nu'}(\mathbf{k},\mathbf{k}') a_{00}^{\nu'}(\mathbf{k}') a_{00}^\nu(\mathbf{k}) \langle l200|l'0\rangle c(\beta,\alpha^*) \times \langle l'2m'm(\beta,\alpha^*)|lm\rangle + m_{l'm'lm}^{\nu'\nu}(\mathbf{k}',\mathbf{k}) a_{00}^\nu(\mathbf{k}) a_{00}^{\nu'}(\mathbf{k}') \times \langle l'200|l0\rangle c(\alpha,\beta^*) \langle l2mm(\alpha,\beta^*)|l'm'\rangle], \quad \alpha,\beta = -,z,+ \ . \tag{30}$$

The values $c(\gamma,\alpha)$ and $m(\gamma,\alpha)$ are defined through Eqs. (6) and (7) with $(\beta=+)^* \Longrightarrow (\beta=-)$ and $(\beta=-)^* \Longrightarrow (\beta=+)$ and similarly for α^*. The quantities $\langle l_1 l_2 m_1 m_2 | l_3 m_3 \rangle$ are Clebsch-Gordan coefficients which are defined in the same way as those used by Jackson.[27] Here, as well as in the following, we have found it more convenient to calculate the in-

teractions in the (I^-,I^z,I^+) basis rather than the (I^x,I^y,I^z) basis. In the (I^x,I^y,I^z) basis, the pseudodipolar coupling is traceless like the dipolar interaction. Therefore, a maximum of five parameters are needed to specify the interaction between two spins. Pseudodipolar, as well as the tensor-tensor matrix elements contain contributions from terms like $\int u_l(r)u_{l'}(r)r^{-1}dr$ where $l-l'=0,\pm2$. However, the off-diagonal $(l\neq l')$ radial integrals are small in comparison with the diagonal $(l=l')$ ones and can be neglected. For example, $\int u_l(r)u_{l'}(r)r^{-1}dr$ for $(l,l')=(0,2)$ is two orders of magnitude smaller than those for $(l,l')=(1,1)$ and (2,2).

3. Tensor-tensor

The tensor-tensor interaction, which arises only from the dipolar hyperfine Hamiltonian, can be written as

$$M^{\alpha\beta}_{\mathrm{TT}}(\mathbf{k},\nu,\mathbf{k}',\nu')=\sum_{l,m,l',m',\bar{l},\bar{m},\bar{l}',\bar{m}'} m^{\nu\nu'}_{lml'm'}(\mathbf{k},\mathbf{k}')m^{\nu'\nu}_{\bar{l}'\bar{m}'\bar{l}\bar{m}}(\mathbf{k}',\mathbf{k})\langle l200|l'0\rangle\langle\bar{l}'200|\bar{l}0\rangle$$
$$\times\sum_{\gamma=-,z,+} c(\gamma,\alpha^*)c(\gamma^*,\beta^*)(1-\tfrac{1}{2}\delta_{\gamma,z})\langle l'2m'm(\gamma,\alpha^*)|lm\rangle$$
$$\times\langle\bar{l}2\bar{m}m(\gamma^*,\beta^*)|\bar{l}'\bar{m}'\rangle,\quad \alpha,\beta=-,z,+\ . \tag{31}$$

This coupling mode has, in general, a nonzero trace.

4. Orbital

The orbital interaction between nuclear spins arises from the orbital part of the hyperfine interaction, Eq. (8). We make use of the fact that the wave functions [Eq. (27)] are expanded in terms of the spherical harmonics. We first rewrite $\mathbf{I}\cdot\mathbf{l}$ as $I^zl^z+\frac{1}{2}(I^+l^-+I^-l^+)$. We are then led to calculate angular integrals

$$\langle lm|l^\alpha|l'm'\rangle=\int Y^*_{lm}(\Omega_r)l^\alpha Y_{l'm'}(\Omega_r)d\Omega_r,\quad \alpha=-,z,+\ , \tag{32}$$

which are readily evaluated by using well-known equations.[27] The matrix element for the orbital interaction can now be written as

$$M^{\alpha\beta}_{\mathrm{orb}}(\mathbf{k},\nu,\mathbf{k}',\nu')=\tfrac{1}{2}\sum_{l,m,m',\bar{l}',\bar{m}',\bar{m}} m^{\nu\nu'}_{lmlm'}(\mathbf{k},\mathbf{k}')m^{\nu'\nu}_{\bar{l}'\bar{m}'\bar{l}'\bar{m}}(\mathbf{k}',\mathbf{k})(1+\delta_{\alpha,z})(1+\delta_{\beta,z})$$
$$\times\langle lm|l^{\alpha^*}|lm'\rangle\langle\bar{l}'\bar{m}'|l^{\beta^*}|\bar{l}'\bar{m}\rangle,\quad \alpha,\beta=-,z,+\ , \tag{33}$$

where the spin degrees of freedom have been summed over. In agreement with Ref. 11, we find that the orbital coupling is anisotropic.

We have calculated the various indirect interactions for copper up to nine nearest neighbors by using the above expressions. The program was tested in several ways to make sure that there were no computational mistakes. The integration of the energy denominator in Eq. (25) was tested by a comparison to the free-electron Lindhard function, Fig. 1. The part of the program which computes the matrix elements for the various coupling modes was tested against a paper and pencil calculation in the case when all $m^{\nu\nu'}_{lml'm'}(\mathbf{k},\mathbf{k}')=1$. One further important test for the final results is that the matrix $\underline{A}_{ij}$ describing the interaction between spins i and j, satisfies the general symmetry requirements which were discussed in Sec. II C to within the numerical accuracy of the computer.

IV. RESULTS

A. Ruderman-Kittel interaction

Since the Ruderman-Kittel interaction is the dominant contribution for the indirect coupling and the easiest contribution to evaluate, we have calculated it separately using a fine mesh in $\mathbf{k}$ space. For the other interactions such a fine mesh is proved impractical. The fine mesh consisted of 408 $\mathbf{k}$ points in the $\frac{1}{48}$th section of the first Brillouin zone, giving rise to 2048 tetrahedrons. $A_{\mathrm{RK}}(\mathbf{q})$ of Eqs. (25) and (28), meaning the diagonal element $A^{\alpha\alpha}_{\mathrm{RK}}(\mathbf{q})$, was evaluated at 23 $\mathbf{q}$ vectors along the symmetry lines [100], [110], and [111]. These values were least-squares fit using a nine-shell model. Table I lists the nine $A_{\mathrm{RK}}(\mathbf{r}_{ij})$ which were determined. As can be seen, the values of $A_{\mathrm{RK}}(\mathbf{r}_{ij})$ drop rapidly with increasing distance. Also shown in Table I are our previous nonrelativistic values,[5] a set of values based on the free-electron approximation, and values obtained by Frisken and Miller using a method which emphasized accurate integration of the energy denominator but had less accurate matrix elements.[14,15] Included also is a fifth set of values evaluated with a coarse set of $\mathbf{k}$ points as described in Sec. IV B below.

There are two dimensionless quantities which characterize the overall strength of the RK interaction and have been measured. The R parameter is defined by

$$R=\frac{\sum_j A_{\mathrm{RK}}(\mathbf{r}_{ij})}{(\mu_0\hbar^2\gamma_n^2\rho)}\ , \tag{34}$$

TABLE I. Values of the Ruderman-Kittel coupling strength, $A_{RK}(\mathbf{r})$, from various calculations. The values are listed in units of nK.

	r_{ij}	LWH[a]	FM[b]	Free el.[c]	This work $\pi/8a$ mesh	This work $\pi/4a$ mesh	Expt.
1	(1,1,0)	−11.67	−8.99	−11.60	−12.74	−10.94	
2	(2,0,0)	1.41	1.56	5.18	1.63	1.13	
3	(2,1,1)	−1.31	−0.76	−2.88	−1.88	−1.47	
4	(2,2,0)	0.11	−0.67	−0.36	−0.17	−0.001	
5	(3,1,0)	0.25	0.61	1.47	0.56	0.44	
6	(2,2,2)	0.61	0.34	0.25	0.94	0.89	
7	(3,2,1)	−0.06	−0.13	−0.83	0.08	−0.12	
8	(4,0,0)	−0.18	−0.17	−0.49	−0.35		
9	(4,1,1)			−0.27	−0.03		
R		−0.34	−0.25	−0.42	−0.37	−0.33	−0.42±0.05[d]
Q		0.091	0.070	0.101	0.101	0.086	0.095±0.003[e]

[a]Values from the nonrelativistic calculation of Lindgård, Wang, and Harmon (Ref. 5).
[b]Nonrelativistic values from the most recent calculation of Frisken and Miller (Ref. 14).
[c]Values obtained using the free-electron approximation and normalized to give the experimental value for R.
[d]Reference 28.
[e]Reference 29. The experimental value for Q is given for coupling between unlike nuclei. Here we have scaled it down by 2.5% to give the Q between average moments.

where ρ is the number density. R is related to the average molecular field and has been measured for copper in NMR experiments on highly polarized spins by Ekström *et al.*[28] The negative sign of R, which was found in the experiment, indicates the antiferromagnetic nature of the interaction. The second parameter, here defined as

$$Q=\frac{\left[\sum_j A_{RK}^2(\mathbf{r}_{ij})\right]^{1/2}}{(\mu_0\hbar^2\gamma_n^2\rho)}, \tag{35}$$

is related to the average fluctuating fields. It has been measured in copper in a magic angle spinning NMR experiment by Andrew *et al.*[29] We have listed the parameters R and Q in Table I for the five sets of calculated $A_{RK}(\mathbf{r}_{ij})$ together with the experimental values. Our present values are in excellent agreement with the measurements.

The values of $A_{RK}(\mathbf{r}_{ij})$ for the $\pi/8a$ fine mesh given in Table I include all contributions from the occupied states in bands 1–6 to the unoccupied states in bands 6–9. In view of the slow convergence when considering only the energy denominator,[14] we have extended the calculations to include the unoccupied states in bands 10–20. With matrix elements included, the convergence is much faster. The largest change occurs for the value of A_{RK} (110) which is reduced by 10%. The value of R is reduced by 7%. The LAPW wave functions for bands 10–20 were expanded in a separate energy window centered about 1.5 Ry above E_F. While further convergence tests are desirable, it is not known how accurate the calculated eigenvalues and wave functions are at energies ($E+E_F>3$ Ry) above the Fermi energy. For this reason, there remains an uncertainty in the values given in Table I of about 10%.

B. Anisotropic coupling

The tensor algebra involved in the calculation of the pseudodipolar, tensor-tensor, and orbital contributions to the coupling is quite time consuming so that we have limited the **k**-space summation to only 256 tetrahedrons. The $\underline{A}(\mathbf{q})$ was evaluated at 10 uniformly spaced **q** vectors in the $\frac{1}{48}$th Brillouin zone. Using this mesh of **q** values, a direct Fourier transform was made to obtain the $\underline{A}(\mathbf{r}_{ij})$. Because the **q** vectors are uniformly spaced at $\pi/2a$ intervals, there are a limited number of unique $\underline{A}(\mathbf{r}_{ij})$ which may be determined since

$$\underline{A}[\mathbf{r}_{ij}+(4la,\ 4ma,\ 4na)]=\underline{A}(\mathbf{r}_{ij}),$$

with l, m, n integers. Nevertheless, the values of $\underline{A}(\mathbf{r}_{ij})$ drop rapidly with increasing r_{ij} and the calculated interactions provide a meaningful representation of the anisotropic coupling.

In Table II we list the elements for the total interaction matrix for the different shells of neighbors. The matrices for different $\mathbf{r}_{ij}$ within the same shell may be obtained using the symmetry relationship, Eq. (17). The Ruderman-Kittel interaction is clearly dominant, and we have listed separately this contribution in Table I where it can be seen that, it spite of greatly reduced number of tetrahedrons, the magnitude and **r** dependence of the interaction strength is reasonably well represented. The other contributions, in particular the orbital contributions, can be substantial as evidenced by the variations in the diagonal elements and the values of the off-diagonal elements. To give some idea of how much the various terms contribute, we give, in Table III, a breakdown of the contributions for the first nearest-neighbor interaction matrix. After the RK interaction, the orbital contributions are the largest, as was first suggested by Oja and Kumar,[11]

TABLE II. Values of the elements for the total interaction matrix, Eq. (16), for different values of $\mathbf{r}_{ij}$. The units are in nK.[a]

r_{ij}	$\underline{A}_{ij}^{xx}$	$\underline{A}_{ij}^{yy}$	$\underline{A}_{ij}^{zz}$	$\underline{A}_{ij}^{xy}$	$\underline{A}_{ij}^{xz}$	$\underline{A}_{ij}^{yz}$
(1,1,0)	−12.597	−12.597	−9.428	−1.979	0.000	0.000
(2,0,0)	1.649	1.802	1.802	0.000	0.000	0.000
(2,1,1)	−2.003	−2.005	−2.005	0.172	0.172	−0.249
(2,2,0)	−0.320	−0.320	−0.272	0.442	0.000	0.000
(3,1,0)	0.580	0.487	0.714	−0.008	0.000	0.000
(2,2,2)	0.945	0.945	0.945	0.034	0.034	0.034
(3,2,1)	0.120	0.098	0.117	−0.046	0.026	−0.050
(4,0,0)	−0.350	−0.350	−0.350	0.000	0.000	0.000
(4,1,1)	−0.030	−0.030	−0.030	0.000	0.000	0.000
$R=-0.34$						
$Q=0.092$						

[a]Here, as well as in Table III, we have used the average gyromagnetic ratio of ^{63}Cu and ^{65}Cu weighted by the natural abundancies. The values in this table were obtained by adding the $\pi/8a$ mesh RK interaction results and the $\pi/4a$ anisotropic interaction results. We believe these to be our most accurate values from the calculations.

however, they are at least a factor of 2 smaller than these authors estimated from their calculations based on the spherical approximation for the wave functions.

The full indirect interaction can be characterized by properly defined R and Q parameters. We substitute $A_{\mathrm{RK}}(\mathbf{r}_{ij})\rightarrow\frac{1}{3}\mathrm{Tr}\underline{A}_{ij}$ in Eqs. (34) and (35) to account for the matrix nature. This way, we find $R=-0.34$ and $Q=0.092$. However, it is presently not clear if thereby obtained values can be readily compared with the experimental values, since anisotropic indirect interactions were not considered in the analysis of the measurements.[28,29]

C. Spontaneous nuclear ordering

When nuclear spins are cooled to such a low temperature that the thermal energy is comparable to the interaction energy, a spontaneous nuclear ordering takes place. Ordering has been observed in copper in magnitude susceptibility measurements[1] and, most notably, in a recent neutron-diffraction experiment.[2] The properties of the ordered phase, particularly its spin structure, pose important tests for microscopically calculated coupling constants. In most of the previous work,[30] the indirect interactions have been described by the free-electron RK interaction, with a strength fitted to reproduce the experimental value.[28,29] The RK interaction has recently been calculated by two groups by starting from the *ab initio* electronic structure.[5,14,15] These studies supported the picture of the strongly competing isotropic RK and dipolar interactions. Now we can investigate how this delicate balance is affected by the additional anisotropic coupling modes as calculated from first principles.

TABLE III. Contributions to the first nearest-neighbor interaction matrix $\underline{A}(1,1,0)$. The orbital, pseudodipolar, and tensor-tensor contributions are given for the different wave function angular momentum components which enter the matrix elements of Eq. (9). The units are nK. The calculations are all done on a $\pi/4a$ mesh.

	$\underline{A}^{xx}$	$\underline{A}^{zz}$	$\underline{A}^{xy}$
RK	−10.94	−10.94	0.00
orb *pp pp*	−0.27	−0.45	0.23
pp dd	1.60	1.93	−0.96
dd dd	−0.86	1.22	−0.68
PD *ss pp*	−0.17	0.33	−0.48
ss dd	−0.16	0.31	−0.11
ss sd	0.00	0.00	0.00
TT *pp pp*	0.05	0.00	0.06
pp dd	−0.07	0.07	−0.12
dd dd	0.01	−0.10	0.09
sd— (*pp,dd,sd*)	0.00	0.00	0.00

We discuss the ordered spin structure by using the mean-field (MF) theory, which has previously been used in this context.[31,32] The ordering in the MF theory takes place through a second-order transition. Therefore, the MF equations can be linearized at the transition temperature and the task of finding the ordering wave vector $\mathbf{Q}_0$ and the critical temperature T_c can be formulated as an eigenvalue problem

$$\underline{A}^{\mathrm{tot}}(\mathbf{q})\cdot\mathbf{e}_n(\mathbf{q})=\lambda_n(\mathbf{q})\mathbf{e}_n(\mathbf{q}),\quad n=1,2,3\ , \tag{36}$$

where $\lambda_n(\mathbf{q})$, $n=1,2,3$ are the eigenvalues and $\mathbf{e}_n(\mathbf{q})$ are the corresponding eigenvectors, which determine the spin polarization. The matrix $\underline{A}^{\mathrm{tot}}(\mathbf{q})$ is a Fourier lattice sum, defined as in Eq. (24), of the total nuclear spin-spin interaction $\underline{A}_{ij}^{\mathrm{tot}}$, which is the sum of the indirect coupling terms Eq. (16) and the direct nuclear dipolar interaction. The Fourier sum of the dipolar part of $\underline{A}_{ij}^{\mathrm{tot}}$ is calculated by using Ewald's method.[33] The ordering wave vector $\mathbf{Q}_0$ corresponds to the wave vector yielding the largest eigenvalue $\lambda_{\max}=\lambda_n(\mathbf{Q}_0)$. Because of crystal symmetry, all vectors belonging to the star of $\mathbf{Q}_0$ are equivalent and hence the ordered structure shows degeneracy. The critical temperature is related to $\lambda_{\max}$ through

$$k_B T_c^{\mathrm{MF}}=\tfrac{1}{3}I(I+1)\lambda_{\max}\ . \tag{37}$$

Therefore, $\lambda_{\max}$ corresponds to the largest critical temperature.

In Fig. 2, we have plotted the quantity

$$T(\mathbf{q}) \equiv \frac{\frac{1}{3}I(I+1)\max[\lambda_1(\mathbf{q}),\lambda_2(\mathbf{q}),\lambda_3(\mathbf{q})]}{k_B} \tag{38}$$

as a function of $\mathbf{q}$ in the high symmetry directions of $\mathbf{q}$ space. The maximum of $T(\mathbf{q})$ is obtained at

$$\mathbf{q}=\mathbf{Q}_0=(2\pi/a)(0.87,0,0)$$

resulting in $T_c^{\mathrm{MF}}=170$ nK.

This mean-field value for T_c is considerably higher than the observed T_c of 58 nK. This is because the frustration inherent in the fcc lattice results in strong fluctuations and thereby lowers T_c as was first shown by Kumar *et al.*[34] More recent calculations and numerical simulations, which make use of the calculated RK interaction, are able to account for the observed T_c.[5,35,36]

The spin polarization corresponding to the ordering wave vector $\mathbf{Q}_0$ is perpendicular to $\mathbf{Q}_0$ and gives rise to a helical spin structure, as has been discussed previously in this context.[37] It is important to note, however, that $T(\mathbf{q})$ along the (100) direction is very flat near the zone boundary, with the zone-boundary value at $(2\pi/a)(1,0,0)$ being only 0.6% lower than at $\mathbf{Q}_0$. With the theoretical uncertainty in the coupling constants arising from a coarse mesh of $\mathbf{k}$ points sampled for the anisotropic terms, limits on band summation, and the neglect of conduction electron spin-orbit coupling, we are unable to make a precise determination of the ordering vector along the $(\xi,0,0)$ direction for ξ between 0.8 and 1.0. Notice that the RK interaction alone gives the ordering wave vectors at $\xi=1$ as shown in Fig. 2. Thus our results suggest that the anisotropic interactions tend to destabilize the ordering at $(2\pi/a)(1,0,0)$. This was also the conclusion of Oja and Kumar, although their use of "spherical" wave functions tended to overestimate the importance of the anisotropic coupling.[11]

For other studies which employed the free-electron form of the RK interaction,[31,32] and also for the nonrelativistic calculations of the RK interaction,[5] the ordering wave vector $\mathbf{Q}_0$ was found to be $(2\pi/a)(1,0,0)$. This is also the ordering wave vector that was found by neutron scattering experiments for both low external magnetic fields and for higher fields that were less than the critical field for the polarized state.[2] While the extremely small difference in energy between our calculated state at $\mathbf{Q}_0$ and the observed state at $(2\pi/a)(1,0,0)$ means that numerical noise may be responsible for the discrepancy, it is prudent to ask if there is perhaps some physics that has been left out. We can see no compelling reason that correlation effects beyond the mean-field theory would tend to stabilize the $(2\pi/a)(1,0,0)$ structure. Higher-order terms in the Hamiltonian might provide the necessary tendency for the wave vector to lock in at the zone boundary, since it would take so little energy. Spin-orbit coupling of the conduction electron would supply a coupling between the electron spins and the lattice and thus might also provide a small energy favoring a zone-boundary wave vector. It is clear that calculations of anisotropic interactions with better numerical accuracy are needed, and it would be worthwhile to further consider mechanisms which might stabilize the zone-boundary ordering wave vector.

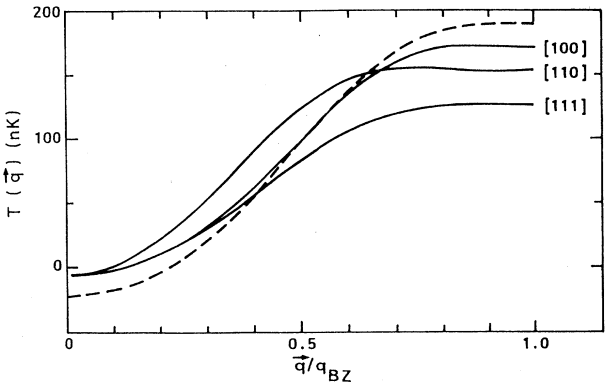

FIG. 2. "q-dependent critical temperature" $T(\mathbf{q})$, as defined by Eq. (38) in the high symmetry directions of the $\mathbf{q}$ space. At the ordering wave vector, $T(\mathbf{q})$ obtains its maximum value which equals the critical temperature. Solid line: dipolar and all indirect interactions. Dashed line: dipolar and RK interactions for the [100] direction.

V. DISCUSSION

The recent experimental achievements in nuclear ordering at low temperatures, particularly in copper, motivated the present work. The Hamiltonian coupling the nuclear spins is relatively simple, which suggests that nuclear magnetism may provide interesting systems allowing detailed comparisons between theory and experiment. In this paper, we have used copper as a prototype system to show how the full indirect coupling strengths can be evaluated from first principles. Where we have been able to make comparisons with experiment, the agreement has been very good, suggesting that similar calculations would be worthwhile for other metals being considered experimentally. Among these metals are Ag,[38] Tl,[39] Pr,[40] and several Pr compounds.[41] While the larger atomic number of these metals means the relativistic mass enhancement will cause the contact and hence, the isotropic RK interaction to be dominant, there also arises the difficulty of assessing the importance of the stronger spin-orbit coupling of the conduction electrons. A full relativistic treatment is probably required and could be carried out with methods similar to those used for atomic hyperfine calculations.[13] For copper we found relativistic corrections to be important, although mainly for the mass enhancement and the resulting changes in the s components of the wave functions near the nucleus. The form of the relativistic matrix elements in terms of the large and small components of the wave functions was also found to be important.

We have discussed the symmetry properties of the coupling matrices, $\underline{A}(\mathbf{r}_{ij})$, and in Appendix A we emphasize that the common practice of decomposing $\underline{A}_{ij}$ into isotropic (RK) and dipolelike parts is, in general, incorrect.

The anisotropic part need not be dipolelike; indeed for fcc or hcp metals the differences may be significant enough that line shape measurements on platinum, lead,[42] and thallium[43] should be reanalyzed in terms of the general symmetry conditions imposed on $\underline{A}_{ij}$. The different components of $\underline{A}_{ij}$ for nearest neighbors may also be determined by performing NMR measurements on single crystals using different directions of the magnetic field with respect to the crystalline axis.

Two other metals which deserve renewed attention are Rb and Cs. These metals are bcc and therefore the nearest-neighbor coupling can be decomposed into RK and terms with dipolelike symmetry. It is, therefore, surprising to find an order of magnitude disagreement between theoretical and experimental values of the dipolelike coupling.[44] We suspect this discrepancy may be resolved by including in $H^{\rm orb}$, all the anisotropic terms some of which were thought to vanish in the earlier theoretical work.[44] The discrepancy certainly points to an interesting case for further study.

Finally, we would like to mention that magnetic susceptibility measurements suggest there is one and possibly two phase transitions between different antiferromagnetic phases which take place in Cu as the magnetic field is increased. The spin configurations for these phases have been the subject of several recent investigations.[8,35,36,45] These theories, which go beyond the mean-field approach presented in this paper, could readily adopt our new values for the coupling constants, including the anisotropic contributions. We expect that the calculated phase boundaries, especially for the phase at intermediate fields if it is confirmed, will be sensitive to the details of the assumed coupling parameters. With further neutron scattering experiments planned, new materials being studied, and new theoretical approaches being applied, the study of nuclear ordering in metals promises to been an exciting field for the future.

ACKNOWLEDGMENTS

We are indebted to Dr. P.-A. Lindgård for his initiation and collaboration on the nonrelativistic calculation of the RK interaction,[5] and for his continued interest and support of the work reported in this paper. We would also like to thank Paul Lane for his assistance in some of the numerical calculations. A.O. is grateful for the warm hospitality of Ames Laboratory and wishes to thank the Finnish Cultural Foundation for travel funds. Ames Laboratory is operated by Iowa State University under Contract No. W-7405-Eng-82. This work was supported by the Director for Energy Research, Office of Basic Energy Sciences. The international collaboration of this research was greatly facilitated by the use of BITNET.

APPENDIX A: NMR ABSORPTION LINE BROADENING

In this appendix, we consider the consequences of the full interaction symmetry (Sec. II C) on the interpretation of NMR line broadening. Several different NMR techniques have been used to obtain information about indirect interactions.[30] The cw NMR line shape itself contains significant information about the nuclear spin-spin interactions. In his classical paper Van Vleck showed how one can exactly calculate various moments of the absorption line.[46] When his results are combined with the theory of Anderson and Weiss,[47] one can estimate the magnitudes of the indirect interactions from the measured line width at half maximum intensity. Assuming isotropic and dipolelike interactions between neighboring spins, two coupling parameters have been extracted from line-shape measurements for Tl,[43] and for Rb and Cs.[48] The coupling parameters have been determined also in Pb and Pt using spin-echo techniques.[42,49] Since all the above mentioned measurements assume that the anisotropic coupling has a dipolelike symmetry rather than a symmetry determined by the crystal (see Sec. II C), it would seem worthwhile to reinvestigate the validity of these analyses.

Here we briefly outline only the calculation of the second moment of the absorption line and point out the form it should take in general. Assuming the magnetic field $\mathbf{B}\|\hat{\mathbf{z}}$ to be so large that the different harmonics are well separated, the second moment of the absorption line is given by

$$\langle \Delta\nu^2 \rangle = -h^{-2}\mathrm{Tr}\{[H^{\rm trunc},I^x]^2\}/\mathrm{Tr}\{(I^x)^2\} , \quad \text{(A1)}$$

where $I^x=\sum_j I_j^x$. $H^{\rm trunc}$ is the so-called truncated Hamiltonian (i.e., the part which commutes with $\sum_j I_j^z$). It is easily shown that an isotropic interaction commutes with I_j^z, and thus only the anisotropic part contributes to $\langle \Delta\nu^2 \rangle$. If the anisotropic coupling has a dipolelike symmetry, one obtains[46]

$$\langle \Delta\nu^2 \rangle = \tfrac{3}{5}h^{-2}I(I+1)\sum_j B_{ij}^2 , \quad \text{(A2)}$$

where $B_{ij}=B(r_{ij})$ is the range function of the dipolelike coupling. For the dipolar interaction, $B_{ij}=\hbar^2\gamma^2/r_{ij}^3$. Equation (A2) holds for a polycrystalline sample, i.e., an average over the magnetic field directions has been taken. If the anisotropic coupling is not required to have a dipolelike symmetry but the general form of Eq. (16) is allowed instead, we find

$$\langle \Delta\nu^2 \rangle_{\rm av} = \tfrac{1}{15}h^{-2}I(I+1)\sum_j [a_{ij}^2+b_{ij}^2+c_{ij}^2-a_{ij}b_{ij}-a_{ij}c_{ij}-b_{ij}c_{ij}+3d_{ij}^2+3e_{ij}^2+3f_{ij}^2] , \quad \text{(A3)}$$

where we have averaged over the magnetic field directions and used the matrix elements of Eq. (16). This is a generalization of Van Vleck's result, Eq. (A2). If conduction electron mediated anisotropic interactions are not negligible in comparison to the dipolar interaction, one has to use Eq. (A3).

In the previous measurements of isotropic and dipolelike interactions,[40,43,48,49] it has been the usual practice to

neglect more distant than nearest-neighbor interactions. This greatly reduces the number of parameters to be determined. In the sc and bcc lattices, the nearest neighbors are in the ⟨100⟩ and ⟨111⟩ directions, so that the number of independent parameters for indirect coupling is two in both cases, and a decomposition into isotropic and dipolelike interactions can be made. Therefore, if the couplings to more distant than nearest neighbors are indeed negligible, no modification due to the nondipolelike symmetry has to be made. However, in the fcc lattice, three independent parameters are needed to describe nearest-neighbor coupling [a, c, and d in Eq. (18b)]. Since the previous work on Pt and Pb gives only two relationships between these parameters,[42,49] more information is needed to extract the nearest-neighbor coupling constants. Similarly, further work is needed to determine the nearest-neighbor coupling constants in Tl (hcp).[38] NMR measurements on single crystals using different directions of the magnetic field with respect to crystalline axis would probably make it possible to extract the nearest-neighbor coupling constants in these metals.

APPENDIX B

In this appendix, we give the results of our calculation for the spin-lattice relaxation rate in Cu. For a more complete discussion of this topic, the reader is referred to the original paper by Obata[9] and later numerical work by Asada *et al.*[10] and by Ebert *et al.*[20] The formulas to be evaluated include

$$(T_1T)_s^{-1}=\frac{4\pi k_B}{\hbar}[\hbar\gamma_n B_s n_s(E_F)]^2 , \tag{B1}$$

$$(T_1T)_{p,\mathrm{orb}}^{-1}=\tfrac{2}{9}\frac{4\pi k_B}{\hbar}[\hbar\gamma_n B_{\mathrm{orb}}^{p} n_p(E_F)]^2 , \tag{B2}$$

$$(T_1T)_{p,\mathrm{dip}}^{-1}=\tfrac{3}{10}(T_1T)_{p,\mathrm{orb}}^{-1} , \tag{B3}$$

$$(T_1T)_{d,\mathrm{orb}}^{-1}=\tfrac{2}{3}\frac{4\pi k_B}{\hbar}[\hbar\gamma_n B_{\mathrm{orb}}^{d} n_d(E_F)]^2 f(2-\tfrac{5}{3}f) , \tag{B4}$$

$$(T_1T)_{d,\mathrm{dip}}^{-1}=\tfrac{1}{49}\frac{4\pi k_B}{\hbar}[\hbar\gamma_n B_{\mathrm{orb}}^{d} n_d(E_F)]^2(\tfrac{5}{3}f^2-2f+2) , \tag{B5}$$

TABLE IV. Calculated nuclear-spin-lattice relaxation rates for ^{63}Cu, along with the various contributions and angular decomposed density of states at E_F.

	Asada *et al.* (Ref. 10)	Ebert *et al.* (Ref. 19)	This work	
			Nonrel.	Rel.
a (a.u.)		6.827	6.76	6.831
$h\gamma_N$ (10^{-24} cgs)	7.51			
E_F (Ry)	0.651	0.651	0.6315	0.6042
n_s (E_F)	0.271	0.271	0.222	0.2395
n_p (E_F)	0.744	0.744	0.511	0.5092
n_d (E_F)	0.98	0.980	0.9335	0.9933
n_{tot}	1.995	1.995	1.958[a]	2.0603[a]
f	0.62	0.62	0.6027	0.6059
$\phi_s^2(0,E_F)/4\pi$	11.16		13.92	14.94[b]
$\langle r^{-3}\rangle_p$	8.15		11.91	12.31
$\langle r^{-3}\rangle_d$	9.45		9.71	9.87
B_s^{rel} (10^6 Oe)		6.560		7.85
B_s^{nrel}	5.85	5.850	7.31	
B_p^{orb}	1.02	1.020	1.49	1.54
B_d^{orb}	1.18	1.183	1.21	1.23
$(T_1T)^{-1}$				
s,rel		0.612		0.689
s,nonrel	0.491	0.487	0.514	
p,orb	0.025	0.025	0.025	0.026
p,dip	0.008	0.007	0.008	0.008
d,orb	0.107	0.104	0.100	0.117
d,dip	0.008	0.007	0.007	0.008
cp				
Total (nonrel)	0.639	0.630	0.654	
Total (rel)		0.755		0.848
Expt.	0.787	0.787	0.787	0.787

[a]The n_l (E_F) in this column are decomposed inside the muffin-tin sphere and have an interstitial n_0 (E_F) added to get the total. The units for the n_l (E_F) are states/(Ry spin atom).
[b]The corresponding value for the relativistic formulation, see text.

where $n_l(E_F)$, $l=s,p,d$ are the angularly decomposed density of states per spin at the Fermi level, k_B is the Boltzmann constant, γ_n is the gyromagnetic ratio of the nucleus, and f is the ratio of the t_{2g} contribution of $n_d(E_F)$ to the total $n_d(E_F)$. The hyperfine fields are defined by

$$B_s=\frac{8\pi}{3}\mu_B\langle|\psi_s(0)|^2\rangle_{E=E_F}=\frac{8\pi}{3}\mu_B\frac{\phi_s^2(r=0,E_F)}{4\pi}\ , \quad \text{(B6)}$$

where $\phi_s(r,E)$ is the normalized $l=0$ radial function at energy E,

$$B_{\text{orb}}^{p\,(d)}=2\mu_B\langle r^{-3}\rangle_{p\,(d)}\ . \quad \text{(B7)}$$

Note that because of the short range of the interaction, less than 2% error is made by restricting the radial integrals to the muffin-tin sphere as we have done.

We have also estimated the core-polarization contribution based on spin polarized atomic calculations and find it negligible. The dipolar interaction, coupling s and d partial waves, was also estimated and found negligible.

Table IV gives the results of our calculations along with those of Asada *et al.*[10] and Ebert *et al.*[20]

*Present address: Department of Physics, University of California at Berkeley, Berkeley, CA 94720.

[1]M. T. Huiku and M. T. Loponen, Phys. Rev. Lett. **49**, 1288 (1982); M. T. Huiku, T. A. Jyrkkiö, and M. T. Loponen, *ibid.* **50**, 1516 (1983); M. T. Huiku, T. A. Jyrkkiö, J. M. Kyynäräinen, A. S. Oja, and O. V. Lounasmaa, *ibid.* **53**, 1692 (1984).

[2]T. A. Jyrkkiö, M. T. Huiku, O. V. Lounasmaa, K. Siemensmeyer, K. Kakurai, M. Steiner, K. N. Clausen, and J. K. Kjems, Phys. Rev. Lett. **60**, 2418 (1988).

[3]M. A. Ruderman and C. Kittel, Phys. Rev. **96**, 99 (1954)

[4]N. Bloembergen and T. J. Rowland, Phys. Rev. **97**, 1679 (1955).

[5]P.-A. Lindgård, X.-W. Wang, and B. N. Harmon, J. Magn. Magn. Mater. **54-57**, 1052 (1986).

[6]I. Lindgren and A. Rosen, Case Stud. At. Phys. **4**, 93 (1974).

[7]E. R. Andrew and W. S. Hinshaw, Phys. Lett. **43A**, 113 (1973).

[8]H. E. Viertiö and A. S. Oja, Phys. Rev. B **36**, 3805 (1987).

[9]Y. Obata, J. Phys. Soc. Jpn. **18**, 1020 (1963).

[10]T. Asada, K. Terakura, and T. Jarlborg, J. Phys. F **11**, 1847 (1981).

[11]A. S. Oja and P. Kumar, J. Low Temp. Phys. **66**, 155 (1987).

[12]D. D. Koelling and B. N. Harmon, J. Phys. C **10**, 3107 (1977).

[13]L. Armstrong, Jr., *Theory of the Hyperfine Structure of Free Atoms* (Wiley, New York, 1971), p. 73.

[14]S. J. Frisken and D. J. Miller, Phys. Rev. Lett. **57**, 2971 (1986).

[15]B. N. Harmon and X.-W. Wang, Phys. Rev. Lett. **59**, 379 (1987).

[16]J. Bardeen, J. Chem. Phys. **6**, 367 (1937).

[17]A. Abragam, *The Principles of Nuclear Magnetism* (Clarendon, Oxford, 1961), p. 209.

[18]L. Wilk and S. H. Vosko, Phys. Rev. A **15**, 1839 (1977).

[19]V. L. Moruzzi, J. F. Janak, and A. R. Williams, *Calculated Electronic Properties of Metals* (Pergamon, New York, 1978).

[20]H. Ebert, H. Winter, and J. Voitländer, J. Phys. F **14**, 2433 (1984).

[21]C. H. Townes, C. Herring, and W. D. Knight, Phys. Rev. **77**, 852 (1950).

[22]E. R. Andrew, J. L. Carolan, and P. J. Randall, Phys. Lett. **35A**, 435 (1971); Chem. Phys. Lett. **11**, 298 (1971).

[23]R. E. Walstedt and Y. Yafet, Solid State Commun. **15**, 1855 (1974).

[24]P.-A. Lindgård, Solid State Commun. **16**, 481 (1975).

[25]J. Rath and A. J. Freeman, Phys. Rev. B **11**, 2109 (1975).

[26]D. D. Koelling and G. O. Arbman, J. Phys. F **5**, 2041 (1975).

[27]J. D. Jackson, *Classical Electrodynamics* (Wiley, New York, 1975).

[28]J. P. Ekström, J. F. Jacquinot, M. T. Loponen, J. K. Soini, and P. Kumar, Physica **98B**, 45 (1979).

[29]E. R. Andrew, J. L. Carolan, and P. J. Randall, Phys. Lett. **37A**, 125 (1971).

[30]A. S. Oja, Phys. Scr. **T19**, 462 (1987).

[31]L. H. Kjäldman and J. Kurkijärvi, Phys. Lett. **71A**, 454 (1979).

[32]P. Kumar, J. Kurkijärvi, and A. S. Oja, Phys. Rev. B **31**, 3194 (1985); **33**, 444 (1986).

[33]G. J. Bowden and R. G. Clark, J. Phys. C **14**, L827 (1981).

[34]P. Kumar, M. T. Loponen, and L. H. Kjäldman, Phys. Rev. Lett. **44**, 493 (1980).

[35]S. J. Frisken and D. J. Miller, Phys. Rev. Lett. **61**, 1017 (1988).

[36]H. E. Viertiö and A. S. Oja (unpublished).

[37]A. S. Oja and P. Kumar, Physica **126B**, 451 (1984).

[38]A. S. Oja, A. J. Annila, and Y. Takano (unpublished).

[39]G. Eska and E. Schuberth, Jpn. J. Appl. Phys. Suppl. **26-3**, 435 (1987).

[40]S. Kawarazaki, N. Kunitomi, J. R. Arthur, R. M. Moon, W. G. Stirling, and K. A. McEwan, Phys. Rev. B **37**, 5336 (1988); K. A. McEwen and W. G. Stirling, Physica B (to be published).

[41]H. Suzuki, M. Namburdribad, B. Bleaney, A. L. Allsop, G. J. Bowder, I. A. Campell, and N. I. Stone, J. Phys. (Paris) Colloq. **C-6**, 801 (1978); J. Babcock, J. Kiely, T. Manley, and W. Weyhmann, Phys. Rev. Lett. **43**, 380 (1979); M. Kubota, H. R. Folle, Ch. Buchal, R. M. Mueller, and F. Pobell, *ibid.* **45**, 1812 (1980); M. Kubota, K. J. Fischer, and R. M. Mueller, Jpn. J. Appl. Phys. Suppl. **26-3**, 427 (1987).

[42]H. Alloul and C. Froidvaux, Phys. Rep. **163**, 324 (1967).

[43]Yu. S. Karimov and I. F. Shchegolev, Zh. Eksp. Teor. Fiz. **91**, 1082 (1961) [Sov. Phys.—JETP **14**, 772 (1962)].

[44]S. D. Mahanti and T. P. Das, Phys. Rev. **170**, 426 (1968); Phys. Rev. B **4**, 46 (1971), and references therein.

[45]P.-A. Lindgård, Phys. Rev. Lett. **61**, 629 (1988).

[46]J. H. Van Vleck, Phys. Rev. **74**, 1168 (1948).

[47]P. W. Anderson and P. R. Weiss, Rev. Mod. Phys. **25**, 269 (1953).

[48]J. Poitrenaud, J. Phys. Chem. Solids **28**, 161 (1967).

[49]C. Froidevaux and M. Weger, Phys. Rev. Lett. **12**, 123 (1964).